Available online at www.sciencedirect.com
ScienceDirect
Journal of the European Ceramic Society 31 (2011) 1123–1130
www.elsevier.com/locate/jeurceramsoc

Original Article

Environmental durability of slurry based mullite–gadolinium silicate EBCs on silicon carbide

Sivakumar Ramasamy [a,*], Surendra N. Tewari [a], Kang N. Lee [b], Ramakrishna T. Bhatt [c], Dennis S. Fox [c]

[a] *Cleveland State University, 2121 Euclid Avenue, Cleveland, OH, USA*
[b] *Rolls-Royce Corporation, P.O. Box 420, Indianapolis, IN, USA*
[c] *NASA Glenn Research Center, 21000 Brook Park Rd., Cleveland, OH, USA*

Received 11 June 2010; received in revised form 3 December 2010; accepted 14 December 2010
Available online 16 January 2011

Abstract

Water vapor oxidation and salt corrosion resistances of mullite–gadolinium silicate (Gd_2SiO_5) environmental barrier coatings (EBCs) dip coated on α-SiC substrates and sintered to 1430 °C/3 h in air were investigated. The EBC exhibited excellent adherence to the substrate during thermal cycling between 1350 °C and room temperature (RT) for 100 h in a simulated lean combustion environment (90% H_2O–balance O_2),[11,13,15] forming ∼10 μm porous silica layer at coating-substrate interface, compared to ∼17 μm for uncoated α-SiC exposed under same conditions. The EBC did not spall after a 24 h 1200 °C exposure in Na_2SO_4 corrosion environment leading to further coat densification. However, after 48 h salt exposure, the EBC showed severe through-thickness cracks, and cavities and de-lamination at coating-substrate interface. The corrosion gaseous products such as CO_2, CO and SO_2 trapped under a low viscosity glassy ($Na_2O{\cdot}x(SiO_2)$) liquid phase were formed due to salt vapor reaction with α-SiC substrate created these cavities.

Keywords: Mullite; Environmental barrier coating; Oxidation resistance; Corrosion; Engine components

1. Introduction

Owing to their oxidation resistance, low density and high temperature strength, SiC fiber reinforced SiC (SiC/SiC) composites have been studied for use in advanced gas turbine engines.[1–4] At high temperatures in dry air or oxygen, the SiC/SiC composite reacts with oxygen that form a thin protective silica (SiO_2) layer preventing from further oxidation. However, in combustion environment, the water vapor present reacts with the SiO_2 layer to form volatile silicon hydroxide ($Si(OH)_4$) leading to severe surface recession depending on the temperature of exposure and velocity of combustion gases.[5–7] Furthermore, when these engines operate under certain applications such as in marine, sodium salt present in the environment reacts with sulfur impurities in the fuel during combustion to form sodium sulphate (Na_2SO_4) that gets deposited on the engine components. Earlier hot corrosion studies on monolithic ceramics[8–10] reveal that the Na_2SO_4 dissolves protective SiO_2 layer, accelerates the oxidation and leads to formation of thick Na–O–Si ($Na_2O{\cdot}x(SiO_2)$) glassy liquid on the surface of the substrate and extensive cavities at the substrate coating interface. To improve the resistance to water vapor oxidation and hot corrosion in combustion environments, protective environmental barrier coatings (EBCs) that hermetically shield the substrate from water vapor and salt attacks are vital to improve environmental durability of silicon-based (SiC/SiC) ceramic engine components.

Mullite[2,11,12] or mullite-based ceramics[13,14] are the most studied EBCs for silicon (Si) based materials such as SiC or SiC/SiC ceramic matrix composites due to their close coefficient of thermal expansion (CTE) match (SiC or SiC/SiC ∼4.5–5.5 × 10^{-6}/°C and mullite ∼5.1 × 10^{-6}/°C).

* Corresponding author. Tel.: +1 216 523 7280; fax: +1 216 687 9220.
E-mail addresses: s.ramasamy1@csuohio.edu, rshiku@yahoo.com (S. Ramasamy).

0955-2219/$ – see front matter © 2010 Elsevier Ltd. All rights reserved.
doi:10.1016/j.jeurceramsoc.2010.12.015

The state-of-the-art EBC applied by the air plasma spraying process to protect these Si based components consists of a barium–strontium–aluminum–silicate (BSAS) topcoat, an intermediate mullite layer, and a silicon bond-coat layer. These mullite/BSAS EBCs, however, form a low melting point glass when BSAS reacts with SiO_2 formed due to oxidation thereby limiting the service temperature less than 1300 °C. Recently, mullite/rare-earth based EBCs have been investigated,[15] which exhibited a better durability and less volatility than the state-of-the-art mullite/BSAS EBCs. We have presented dense slurry based mullite/rare-earth (gadolinium silicate, Gd_2SiO_5) EBCs for SiC and Si_3N_4 ceramics by an inexpensive and versatile dip coating process.[16–18] Further, it was also shown that these EBCs provided enhanced oxidation protection after 1350 °C–room temperature (RT) thermal cycling for up to 400 h when applied on SiC ceramic substrates.[18]

Although it is well understood that salt impurities in combustion environments accelerate the degree of component degradation, most studies until now investigated only cyclic oxidation of EBC coated silicon based materials through thermal cycling experiments. Only limited efforts have been made to evaluate the corrosion resistance of protective EBCs. Lee[19] has shown that air plasma sprayed mullite coatings had a good resistance to crack formation in a combustion environment under thermal cycling between 1000 °C and RT, and to hot corrosion when exposed in a Na_2CO_3 environment at 1000 °C for 24 h.

The objective of this present work was to understand the oxidation as well as corrosion resistance of our slurry based mullite/Gd_2SiO_5 EBCs coated on α-SiC coupons (a model material used for the SiC/SiC composite). The oxidation behavior of mullite/Gd_2SiO_5 EBCs was evaluated under simulated combustion environment by thermal cycling between 1350 °C and RT for 100 h exposure. Further, the corrosion resistance of EBC coated α-SiC coupons was investigated at an elevated temperature of 1200 °C for up to 48 h in Na_2SO_4 salt environment. The damage after Na_2SO_4 induced corrosion of mullite/Gd_2SiO_5 EBC coated specimens examined was compared with moisture induced damage during thermal cycling.

2. Experimental procedure

2.1. Materials and processing

Sintered α-SiC (Hexaloy™, Saint Gobain Ceramics, Niagara Falls, NY) coupons were used as the coating substrates. Alcohol based mullite/Gd_2SiO_5 slurries were coated on these substrates by an in-expensive dip coating process followed by air sintering to 1430 °C for 3 h. Our preliminary results[20] indicated that a combination of mullite powder, polyvinyl butyral (PVB), phosphate ester (PE), and ethyl alcohol as binder, dispersant and solvent, respectively, was effective to develop mullite based slurries. To ensure molecular level mixing of a starting materials, powders of mullite (d_{72}: 3 μm, Baikowski International Corporation, USA) and Gd_2SiO_5 (d_{50}: 0.9 μm, Praxair Surface Technologies, USA) mixed at 88/12 wt.% were mechanically alloyed in a planetary mill (30-min, zirconia vial, zirconia balls). Prior to powder addition, 4 wt.% of PVB (Sigma, USA) and 0.6 wt.% of PE (Sigma, USA) was added to ethanol (>99.5% pure, Sigma–Aldrich, USA) and mixed well using a magnetic stirrer. The slurry containing solid–liquid mixture with ratio of 1:2 was then mixed for a period of 12 h. Details of the processing parameter optimization, slurry preparation and coating procedures are presented in an earlier paper.[16]

2.2. Thermal cycling

The mullite/Gd_2SiO_5 EBC durability was assessed by exposing the coated SiC coupons to thermal cycling at 1350 °C in 90% H_2O–balance O_2 environment with a flow rate of 2.2 cm/s at 1 atm using an automated thermal cycling furnace described in Ref. 13. Each thermal cycle consisted of transferring the specimen rapidly from the cold zone of the furnace maintained at RT to the hot zone of the furnace maintained at 1350 °C, holding the sample at 1350 °C for 1 h, transferring the specimen quickly to the cold zone and holding the specimen in the cold zone for 15 min at room temperature. The EBC coated α-SiC coupons were exposed to 100 thermal cycles. For comparison purpose, un-coated α-SiC coupons were thermal cycled in the similar combustion environment between 1350 °C and RT for 100 thermal cycles. In addition, un-coated α-SiC coupons were also cycled between 1300 °C and RT for 500 thermal cycles.

2.3. Corrosion

Corrosion tests were carried out on the coated specimens in a horizontal tubular furnace at 1200 °C for up to 48 h. The schematic of the tubular corrosion furnace is depicted in Fig. 1. The platinum crucible with Na_2SO_4 powder was placed in the furnace and maintained at a constant temperature of 1000 °C. Since the melting point of Na_2SO_4 is about 850 °C, the molten salt vaporizes at 1000 °C and the vapors were carried to reaction/hot zone (1200 °C) by argon gas with a flow rate of 100 cc/min. When Na_2SO_4 is heated up to 1000 °C, it generates a 300 ppm vapor concentration of the salt[21] for the given flow rate which decomposes to Na_2O and SO_3. The coated specimens placed on alumina boats were positioned in the hot zone of tubular furnace. After 24 h corrosion, a set of coated coupons were removed from the furnace and remaining specimens were further exposed to 48 h.

2.4. Characterization

Coated coupons after thermal cycling and hot corrosion were mounted in epoxy, sectioned and polished up to 0.05 μm alumina suspension for cross-sectional observations. A scanning electron microscope (SEM, AMRAY 1820, USA) equipped with an energy dispersive X-ray spectrometer (EDX) was utilized to observe coating cross-sections and for elemental analyses. The thickness of oxide layer formed adjacent to the substrates was measured from SEM micrographs. The coating adherence and extent of damage in the substrate/coating interface after thermal cycling and corrosion tests were evaluated through microstructural observation.

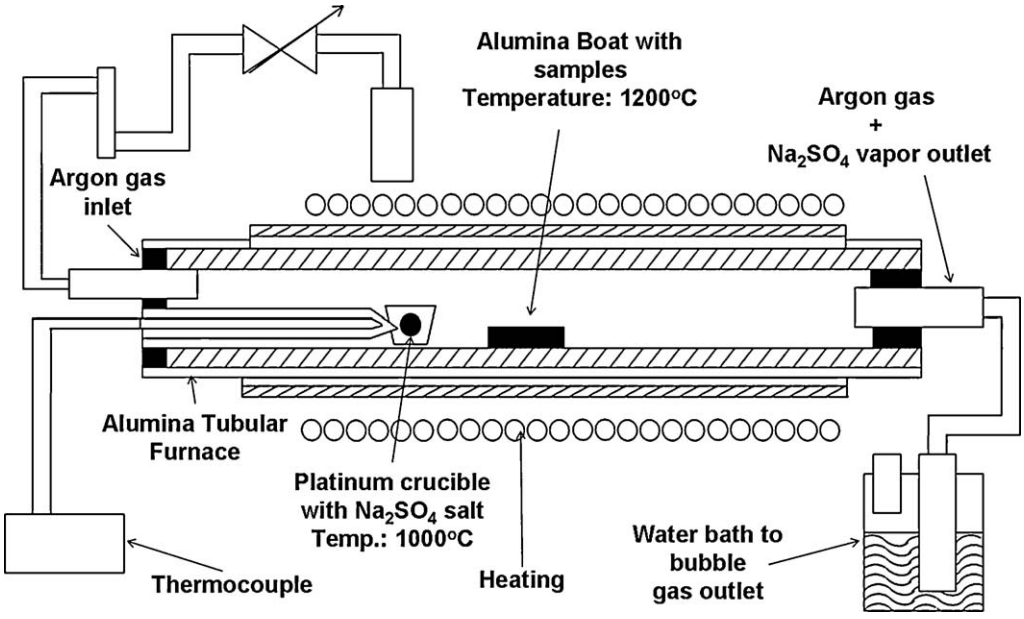

Fig. 1. Schematics of tubular corrosion furnace.

3. Results and discussion

3.1. Coating morphology

Fig. 2(a)–(c) exhibits the SEM cross-sectional morphologies of mullite/Gd_2SiO_5 EBC coated on α-SiC substrate and sintered in air at 1430 °C for 3 h. As depicted in a low magnification views in Fig. 2(a) and (c), the EBC appeared to be adhered well at the chamfered, edge, corner, and flat regions of α-SiC substrate after sintering. However, the coating in the flat regions was always thicker than other regions due to slurry drainage (Fig. 2(c)). In addition, the high magnification cross-sectional images show that gadolinium (Gd) rich phases were uniformly distributed throughout the coating as shown in Fig. 2(b). This magnified image of EBC coating shows two phase type microstructure with mullite particles and the white gadolinium (rich) glassy phase in the inter-particle region. Also, there is some porosity in the sintered coating. However, the pores are not interconnected. Fig. 2(d) shows the EDX elemental analyses across the coating thickness. Each data point corresponds to analysis from 18 μm × 4 μm rectangular regions (typically indicated by the arrow in Fig. 2(a)) across the coat thickness.

3.2. Thermal cycling in moisture

Fig. 3(a) shows the SEM cross-sectional image of un-coated α-SiC substrate after 500 thermal cycles in the moisture containing environment between 1300 °C and RT. A porous silica (SiO_2) scale of about 45–50 μm thick was formed on surface after the thermal cycling due to oxidation of α-SiC by O_2 and H_2O. Cyclic formation and the evaporation of silicon hydroxide ($Si(OH)_4$) is responsible for the rows of aligned pores seen in the oxidized damage-zone. In addition, frequent through thickness cracks formed across the damage-zone, which would be expected to provide direct access of moisture to the substrate below further accentuating SiO_2 formation and damages. Fig. 3(b) shows the nature of moisture induced oxidation of un-coated α-SiC after 100 cycles from 1350 °C to room temperature. For the 1350 °C cycled sample, the porous silica layer is ∼17 μm thick. This is significantly more severe compared to ∼10 μm thick layer after 100 cycles at 1300 °C. There is also evidence of severe and frequent silica scale spallation during 1350 °C to RT cycling as seen in magnified portion of Fig. 3(b). This can be attributed to larger and more interconnected nature of the aligned pores formed during thermal cycling at higher temperature.

Fig. 4(a) and (b) shows the SEM cross-sections of mullite/Gd_2SiO_5 EBC coated on α-SiC substrate after 100 thermal cycles between 1350 °C and RT in 90% H_2O–balance O_2 combustion environment. It is evident from the low magnification image (Fig. 4(a), inset) that after thermal cycling at 1350 °C, the EBC remained intact on α-SiC substrate. In addition, the coating appeared to have densified. The coating underwent sintering and became denser during thermal cycling. Even though water vapor transport is through the coating and its reaction with α-SiC substrate could not be completely stopped, as indicated by the presence of ∼10 μm thick silica layer in Fig. 4(b), the extent and severity of moisture induced damage in the specimens was significantly less compared to the un-coated α-SiC specimens (compare Fig. 3(b) with Fig. 4(b)). This reduced oxidation rate in coated specimens is an indication that the pores in the sintered coating are not interconnected. Fig. 4(c) shows the EDX elemental analyses across the mullite/Gd_2SiO_5 EBC after thermal cycling at 1350 °C for 100 h. The results suggest that after thermal cycling, the Gd_2SiO_5 maintained homogenous distribution in the mullite matrix. The silicon-rich and aluminum-poor profile close to the interface is from the micro-porous SiO_2 layer formed due to oxidation.

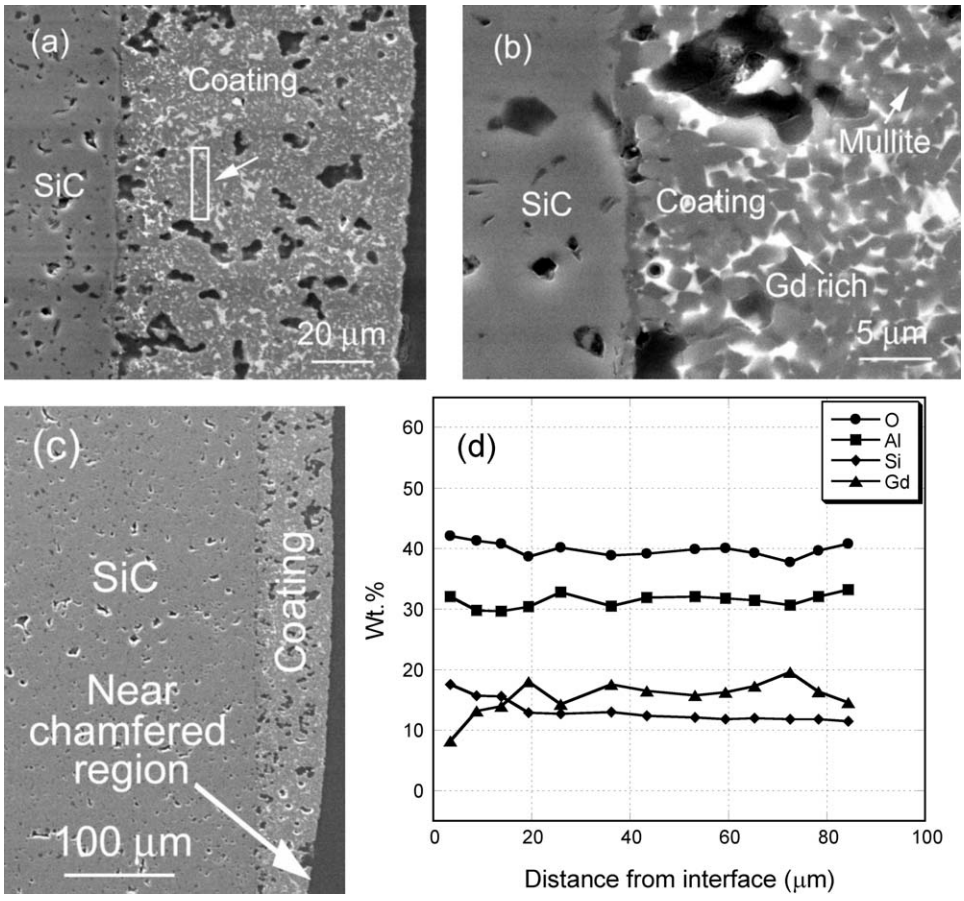

Fig. 2. (a) SEM cross-sectional view of 88 wt.% mullite–12 wt.% Gd_2SiO_5 EBCs coated on α-SiC coupon, (b) high magnification SEM cross-section indicating coating-substrate interface, (c) SEM cross-section near chamfered region showing the decrease in coating thickness due to slurry drainage, and (d) EDX elemental analysis across the coating that confirms uniform dispersion of Gd_2SiO_5 in mullite matrix.

3.3. Salt corrosion

Fig. 5(a) is an optical surface image of mullite/Gd_2SiO_5 EBC coated α-SiC sample after 24 h exposure at 1200 °C in Na_2SO_4 salt environment. The bottom and top regions, showing cavities in Fig. 5(a), correspond to the chamfered edge portions of the sample where the coating is much thinner than on flat side surfaces. It is evident that the EBC maintained excellent adherence

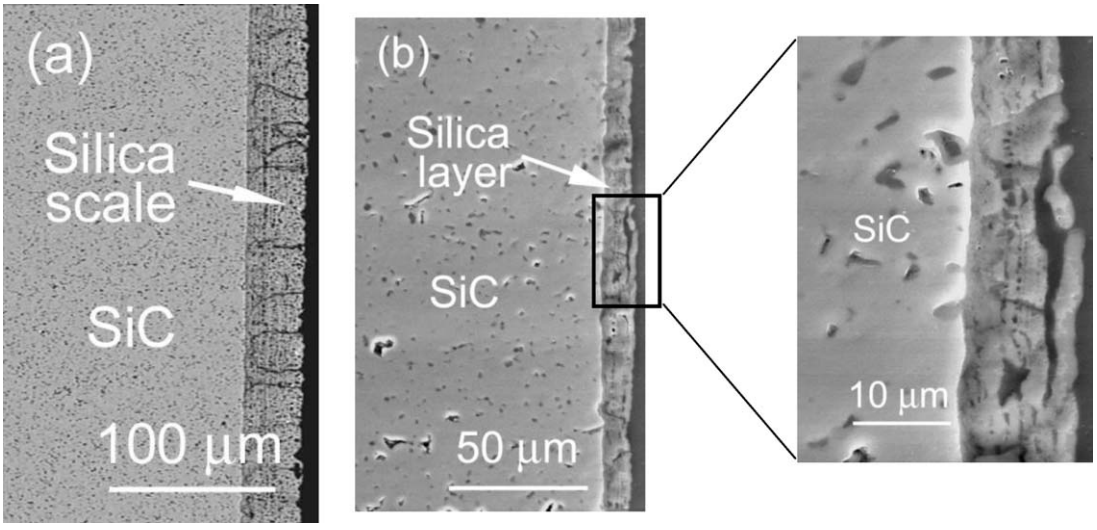

Fig. 3. SEM cross-sections of bare α-SiC after thermal cycling in the lean combustion environment: (a) between 1300 °C and room temperature (RT) for 500 h and (b) between 1350 °C and RT for 100 h.

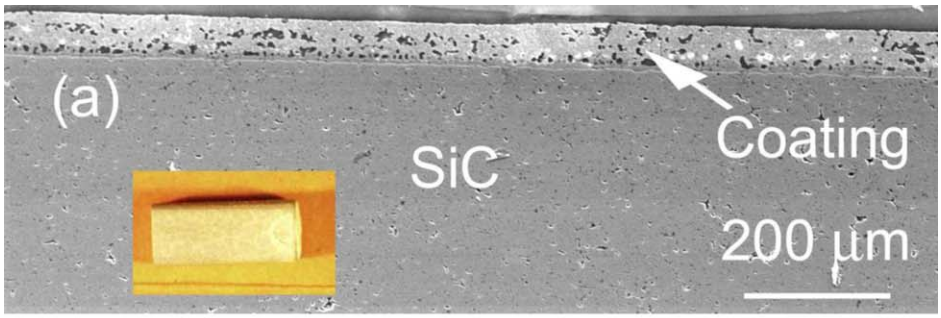

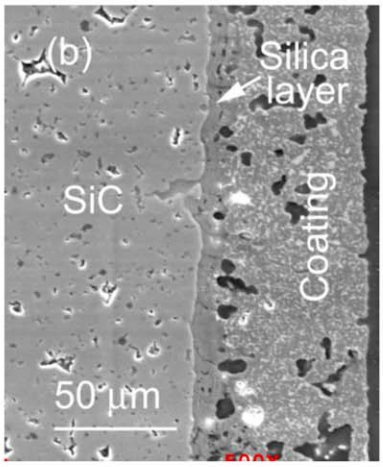

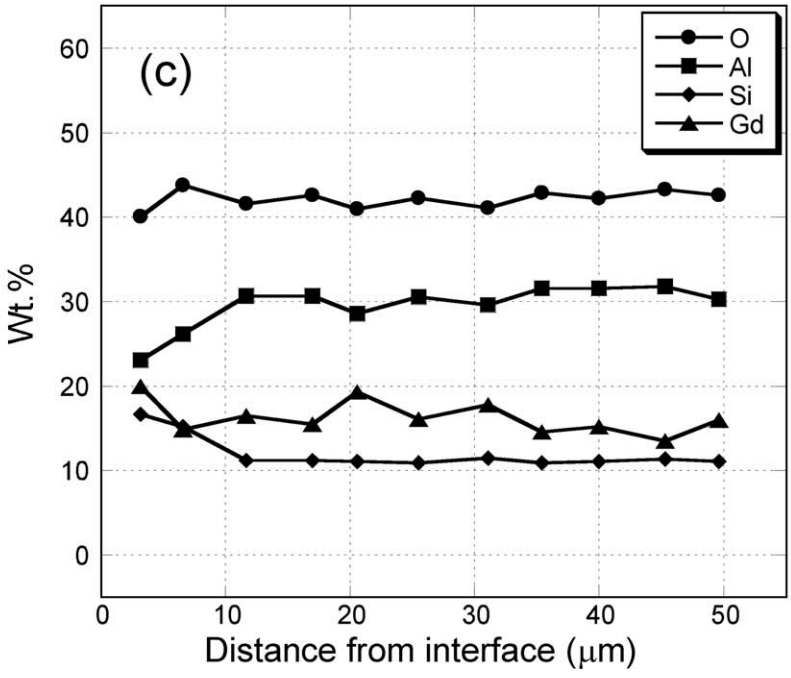

Fig. 4. (a) Low magnification SEM cross-sectional view of 88 wt.% mullite–12 wt.% Gd_2SiO_5 EBCs coated on α-SiC coupon after thermal cycling in the simulated combustion environment between 1350 °C and room temperature for 100 h. The inset is the overall image of thermal cycled coated coupon that reveals excellent coating adherence, (b) SEM cross-section after 1350 °C thermal cycling indicating moisture induced oxidation damages at coating-substrate interface with an silica layer of ∼10 μm, and (c) EDX elemental analysis across the coating that shows SiO_2 buildup near the coating-substrate interface with uniform dispersion of Gd_2SiO_5 in mullite matrix.

to the substrate on the flat-sides of the sample after salt exposure. Macro cracks were seen to be developing on the surface and these are believed to be caused by the significant coating densification occurring during high temperature salt exposure. However, these cracks were present only on the surface and did not penetrate across the coating thickness, as verified by the cross-sectional SEM views along the sample length (typically shown in Fig. 5(b)).

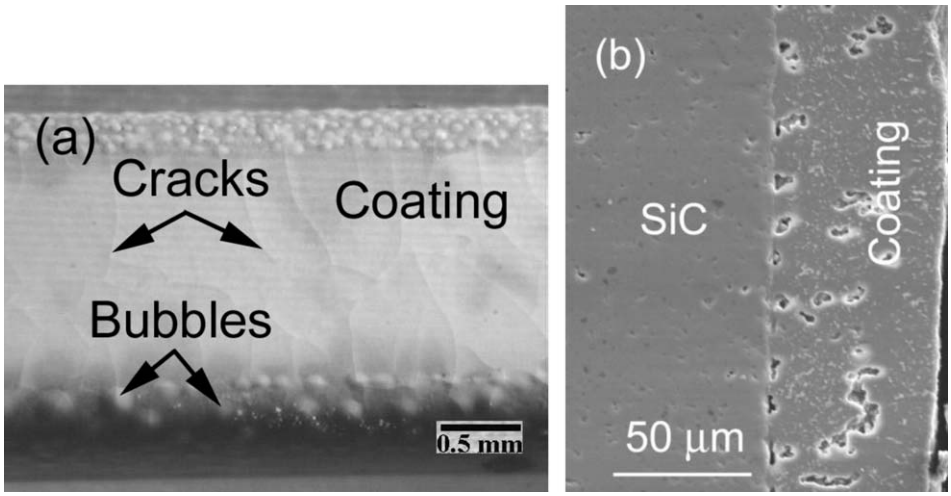

Fig. 5. (a) Optical view of mullite/Gd_2SiO_5 EBC coated on α-SiC coupon after 24 h Na_2SO_4 exposure at 1200 °C showing bubbles in chamfered region and surface cracks and (b) SEM cross-sectional views revealing a substantial coating densification with excellent adherence to substrate.

The coating has become significantly denser after 24 h exposure at 1200 °C when exposed to Na_2SO_4 salt vapor (Fig. 5(b)). This enhanced coating densification can be attributed to the diffusion of salt and its reaction with the coating constituents. As the melting point of Na_2SO_4 is 884 °C,[21] at high temperatures than melting point, Na_2SO_4 disintegrates into Na_2O and SO_3, both in gaseous forms. As mullite is well known to be a good conductor of sodium,[22,23] sodium oxide (Na_2O) diffuses in coating and react with mullite to form $Na_2O{\cdot}Al_2O_3{\cdot}2SiO_2$. The main reactions involved in this Na_2SO_4 salt vapor corrosion are given below:

$$Na_2SO_{4(l)} = Na_2O_{(g)} + SO_{3(g)} \quad (1)$$

$$Na_2O_{(g)} + (3Al_2O_3{\cdot}2SiO_2) = Na_2O{\cdot}Al_2O_3{\cdot}2SiO_2 + 2Al_2O_3 \quad (2)$$

It is interesting to note that un-coated α-SiC when exposed to Na_2SO_4 salt vapor environment only at 1000 °C for 48 h, the silica (SiO_2) layer formed on α-SiC surface during oxidation reacts with sodium oxide to form a uniform silicate ($Na_2O{\cdot}x(SiO_2)$) glassy layer with extensive cavities throughout its surface.[8] The chemical reaction that forms the low melting point sodium silicate is given below:

$$Na_2O_{(g)} + xSiO_{2(s)} = Na_2O{\cdot}xSiO_{2(l)} \quad (3)$$

The present mullite–gadolinium silicate EBC coating, on the other hand, remained adherent to the α-SiC substrate after 24 h Na_2SO_4 salt vapor exposure at even after exposure at 1200 °C. Fig. 6 shows microstructure of mullite/Gd_2SiO_5 coated α-SiC coupon after 48 h exposure at 1200 °C in Na_2SO_4 salt environment. From the overall optical view in Fig. 6(a) it is evident that substantial amount of glassy corrosion product, with extensive cavities, formed at the coating-substrate interface, which caused the coating to delaminate. As shown in the SEM cross-sectional view of the coating-substrate interface in Fig. 6(b), the coating appears to have densified further during 48 h 1200 °C salt exposure (compare Fig. 2(a) to Fig. 6(b)). This may be attributed to more salt vapor reacting with coating constituents compared to 24 h exposure. In addition, the extensive through thickness cracks developed in the coating provided path for the salt to directly reach the coating-substrate interface. The low melting point glassy ($Na_2O{\cdot}x(SiO_2)$) liquid phase formed due to reaction of salt vapor with the α-SiC substrate is believed to be responsible for extensive cavities at the interface. The corrosion gaseous products such as CO_2, CO and SO_2 trapped under a low viscosity glassy phase create these cavities. Distribution of gadolinium rich particles in the coating also changed after 48 h exposure, region near the substrate interface became denuded and the region near external surface of the coating became enriched (white phase near the surface in Fig. 6(b)).

Fig. 7(a) and (b), respectively, show the results of EDX elemental analyses across the coating after 24 h and 48 h Na_2SO_4 salt corrosion at 1200 °C. Distribution of all the elements examined Na, Al, Si, S, Gd and O, appeared to be reasonably uniform across the entire coating thickness after the 24 h exposure except for the decreased Gd and increased Si content in the immediate vicinity of the interface (Fig. 7(a)). About 0.6–1% sodium and sulfur were observed throughout the coating thickness. The 48 h exposure to salt vapor, however, produced a systematic increase in silicon, oxygen, and sodium content of the coating from its outer surface towards coat-substrate interface (Fig. 7(b)). Gadolinium and aluminum showed the opposite trend. The higher sodium concentration towards substrate suggests that salt vapor access to the interface was not limited only to its ionic transport through the silicate networks in the coating, but it also had direct access to α-SiC through either the transverse cracks in the coating or through fissures along the interface caused by coat de-bonding. Coating near the interface became enriched in sodium silicate because of enhanced oxidation of SiC substrate due to the salt vapor present there. This observation is in agreement with Jacobson and Smialek[8] who reported that the amount of silica formed when α-SiC was kept for 48 h at 1000 °C in Na_2SO_4 vapor environment was 10–20 times larger than when it was oxidized in air. The gadolinium appears to have migrated towards the surface; the reason for this behavior is not clear at this stage.

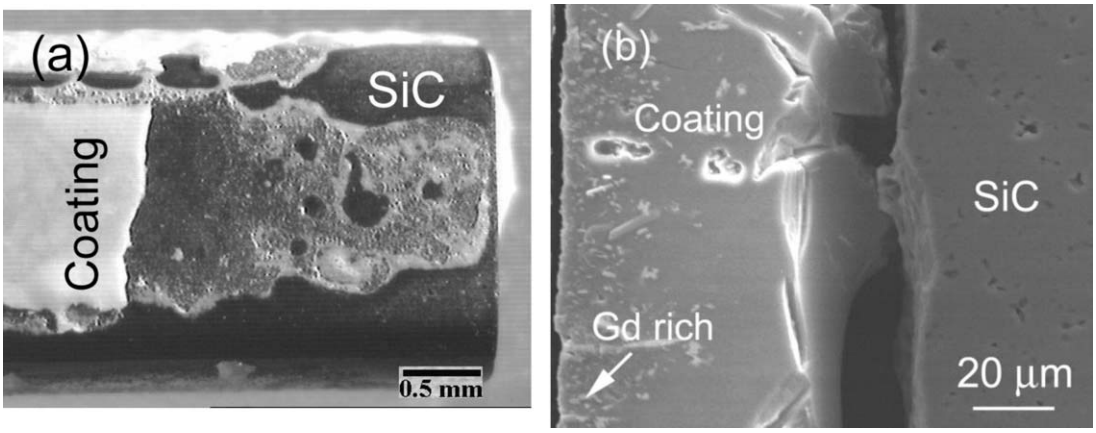

Fig. 6. (a) Optical and (b) SEM cross-sectional views of mullite/Gd_2SiO_5 EBC coated on α-SiC coupon after 48 h Na_2SO_4 exposure at 1200 °C showing extensive bubble formation and coating delamination.

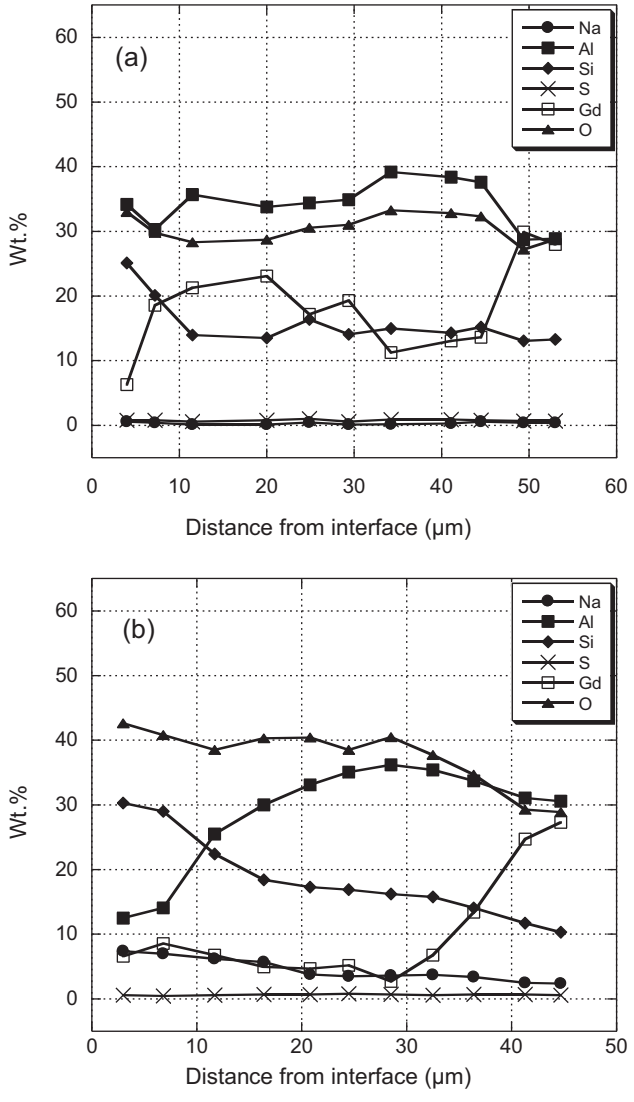

Fig. 7. EDX elemental analyses across the coating after Na_2SO_4 salt exposure (a) for 24 h indicating uniform Na concentration throughout the coating with Gd segregation towards outer edge of coating and (b) for 48 h indicating a gradual increase of Na concentration towards the coating-substrate interface with high Gd segregation towards outer edge of coating.

It is interesting to note that exposure of coated silicon carbide to salt vapor environment is significantly more damaging than compared to the water vapor attack. Coated coupons after thermal cycling in moisture containing environment at 1350 °C for 100 h showed less severe damage when compared to those after Na_2SO_4 corrosion for only 48 h at a much lower temperature of 1200 °C.

4. Conclusion

In this study the environmental durability of slurry based mullite–Gd_2SiO_5 EBCs was investigated by exposing the coated α-SiC coupons to simulated moisture containing combustion as well as salt containing corrosion environments. The EBCs showed an excellent adherence with only about 10 μm silica layer formation at substrate-coating interface after 100 thermal cycles between 1350 °C and room temperature, which suggests that these coatings have outstanding CTE match with α-SiC substrate. Mullite–Gd_2SiO_5 EBCs remained well adherent to substrate protecting against Na_2SO_4 salt environment up to 24 h at 1200 °C. The coating became denser during 1200 °C exposure to the salt. The enhanced salt assisted reactions attributed to modification of silicate network due to sodium oxide resulted in severe through-thickness cracks after 48 h exposure. The low melting point glassy ($Na_2O{\cdot}x(SiO_2)$) liquid phase formed due to reaction of salt vapor with the α-SiC substrate is believed to be responsible for extensive cavities at the substrate-coating interface. The corrosion gaseous products such as CO_2, CO and SO_2 trapped under a low viscosity glassy phase create these cavities, which ultimately lead to coating de-lamination. A systematic increase of silicon, oxygen and sodium content from external coating surface towards the coat-substrate interface, and a decrease of gadolinium and aluminum were observed during salt exposure.

References

1. Jacobson NS. Corrosion of silicon-based ceramics in combustion environments. *J Am Ceram Soc* 1993;**76**(1):3–28.
2. Lee KN, Miller RA, Jacobson NS. New generation of plasma sprayed mullite coatings on silicon carbide. *J Am Ceram Soc* 1995;**78**(3):705–10.

3. Kimmel J, Miriyala N, Price J, More K, Tortorelli P, Eaton H, et al. Evaluation of CFCC liners with EBC after field testing in a gas turbine. *J Eur Ceram Soc* 2002;**22**:2769–75.
4. Lee KN. Current status of environmental barrier coatings for Si-based ceramics. *Surf Coat Technol* 2000;**133–134**:1–7.
5. Opila EJ, Hann Jr RE. Paralinear oxidation of CVD SiC in water vapor. *J Am Ceram Soc* 1997;**80**(1):197–205.
6. Opila EJ. Variation of the oxidation rate of silicon carbide with water–vapor pressure. *J Am Ceram Soc* 1999;**82**(3):625–36.
7. Robinson RC, Smialek JL. SiC recession caused by SiO_2 scale volatility under combustion conditions. I. Experimental results and empirical model. *J Am Ceram Soc* 1999;**82**(7):1817–25.
8. Jacobson NS, Smialek JL. Hot corrosion of sintered α-SiC at 1000 °C. *J Am Ceram Soc* 1985;**68**(8):432–9.
9. Smialek JL, Jacobson NS. Mechanism of strength degradation for hot corrosion of α-SiC. *J Am Ceram Soc* 1986;**69**(10):741–52.
10. Jacobson NS, Kinetics. Mechanism of corrosion of SiC by molten salts. *J Am Ceram Soc* 1986;**69**(1):74–82.
11. Lee KN, Miller RA. Oxidation behavior of mullite-coated SiC and SiC/SiC composites under thermal cycling between room temperature and 1200–1400 °C. *J Am Ceram Soc* 1996;**79**(3):620–6.
12. Krishnamurthy R, Sheldon BW, Haynes JA. Stability of mullite protective coatings for silicon-based ceramics. *J Am Ceram Soc* 2005;**88**(5):1099–107.
13. Lee KN, Fox DS, Eldridge JI, Zhu D, Robinson RC, Bansal NP, et al. Upper temperature limit of environmental barrier coatings based on mullite and BSAS. *J Am Ceram Soc* 2003;**86**(8):1299–306.
14. Lee KN, Eldridge JI, Robinson RC. Residual stresses and their effects on the durability of environmental barrier coatings for SiC ceramics. *J Am Ceram Soc* 2005;**88**(12):3483–8.
15. Lee KN, Fox DS, Bansal NP. Rare earth silicate environmental barrier coatings for SiC/SiC composites and Si_3N_4 ceramics. *J Eur Ceram Soc* 2005;**25**:1705–15.
16. Sivakumar R, Tewari SN, Lee KN, Bhatt RT, Fox DS. EBC development of hot-pressed Y_2O_3/Al_2O_3 doped silicon nitride ceramics. *Mater Sci Eng A* 2010;**527**:5492–8.
17. Sivakumar R, Tewari SN, Lee KN, Bhatt RT, Fox DS. Slurry based multilayer environmental barrier coatings for silicon carbide and silicon nitride ceramics. I. Processing. *Surf Coat Technol* 2010;**205**:258–65.
18. Sivakumar R, Tewari SN, Lee KN, Bhatt RT, Fox DS. Slurry based multilayer environmental barrier coatings for silicon carbide and silicon nitride ceramics. II. Oxidation resistance. *Surf Coat Technol* 2010;**205**:266–70.
19. Lee KN. Key durability issues with mullite-based environmental barrier coatings for Si-based ceramics. *Trans ASME* 2000;**122**:632–6.
20. Chen GF, Lee KN, Tewari SN. Slurry development for the deposition of a $GdSiO_4$ + mullite environmental barrier coating on silicon carbide. *J Ceram Proc Res* 2007;**8**(2):142–4.
21. Cheng L, Xu Y, Zhang L, Luan X. Corrosion of a 3D-C/SiC composite in salt vapor environments. *Carbon* 2002;**40**:877–82.
22. Jacobson NS. Sodium sulphate: deposition and dissolution of silica. *Oxid Met* 1989;**31**:91–103.
23. Jacobson NS, Lee KN. Corrosion of mullite by molten salts. *J Am Ceram Soc* 1996;**79**(8):2161–7.